Inorg. Chem. **2002**, *41*, 6153–6160

Structural, Electronic, and Magnetic Consequences of *O*-Carbonyl vs *O*-Alkoxy Ester Coordination in New Dicopper Complexes Containing the $Cu_2(\mu\text{-}Cl)_2$ Core

Pratibha Kapoor,* Anuradha Pathak, Ramesh Kapoor, and Paloth Venugopalan

Department of Chemistry, Panjab University, Chandigarh 160 014, India

Montserrat Corbella*

Departament de Química Inorgànica, Universitat de Barcelona, Martí i Franquès, 1-11, E-08028 Barcelona, Spain

Montserrat Rodríguez,[†] Juvencio Robles,[‡] and Antoni Llobet*,[†]

Departament de Química and Institut de Química Computacional, Universitat de Girona, Campus de Montilivi E-17071, Girona, Spain

Received March 5, 2002

The complexes $[Cu_2(\mu\text{-}Cl)_2(Cl)_2(L)_2]$ (L = dialkylpyridine-2,6-dicarboxylate; R = Et, L = depc, **1**; R = *i*-Pr, L = dppc, **2**) have been prepared and their magnetic properties studied. The crystal structures of complexes **1** and **2** have been solved. Compound **1** belongs to the $P\bar{1}$ space group with $Z = 2$, $a = 8.3020(10)$ Å, $b = 9.2050(10)$ Å, $c = 10.065(2)$ Å, $\alpha = 99.040(10)°$, $\beta = 100.810(10)°$, and $\gamma = 106.502(10)°$ whereas **2** belongs to the *C*2/*c* space group with $Z = 8$, $a = 11.6360(10)$ Å, $b = 25.906(3)$ Å, $c = 11.76579(10)$ Å, and $\beta = 107.900(10)°$. The different alkyl ester substitutes produce substantial structural and electronic differences. The Cu_2Cl_2 core geometry is planar for **1** whereas it adopts a butterfly shape in the case of **2.** Furthermore, in **2** the dppc ligand coordinates only by the carbonyl oxygen atoms whereas in **1** the depc ligand coordinates through carbonyl and alkoxy oxygen atoms. Magnetic susceptibility data show a ferromagnetic coupling between the two Cu(II) centers in both cases ($J = 39.9(6)$ cm^{-1} for **1**, and $J = 51.3(5)$ cm^{-1} for **2**) with very weak antiferromagnetic interactions ($J' = -0.59$ cm^{-1} and -0.57 cm^{-1} for **1** and **2**, respectively). Theoretical calculations at the extended Hückel level have also been carried out to further understand the electronic nature of complexes **1** and **2**.

Introduction

The magnetic properties of transition metal complexes have received increasing attention over the past decades because of their interest from a basic point of view and also because of their growing body of recent applications.[1]

Of particular interest are dinuclear copper complexes containing the $Cu_2(\mu\text{-}Cl)_2$ core, since their magnetic properties vary drastically depending on the relative geometry of the copper centers and also on the distortions suffered by the core from an ideal geometry.[2]

In the present paper we describe the synthesis, structure, and magnetic properties of two new examples of copper

* Authors to whom correspondence should be addressed. E-mail: antoni.llobet@udg.es (A.L.).

[†] Departament de Química.

[‡] Departament de Química and Institut de Química Computacional. Permanent address: Facultad de Química, Universidad de Guanajuato, Noria Alta s/n, Guanajuato, GTO, 36050, Mexico.

(1) (a) Carlin, R. L. In *Magnetochemistry*; Springer-Verlag: Berlin, Heidelberg, 1986. (b) Reedijk, J. In *Bioinorganic Catalysis*; Marcel Dekker: New York, 1993. (c) Salomon, E. I.; Wilcox, D. E. In *Magneto-structural correlations in exchange coupled systems*; Gatteschi, D., Kahn, O., Willett, R. D., Eds.; NATO Advanced Study Institute Series, Vol. C140; D. Reidel: Dordrecht, Holland, 1984. (d) Cornia, A.; Gatteschi, D.; Sessoli, R. *Coord. Chem. Rev.* **2001**, *219*, 573. (e) Kahn, O. In *Modular Chemistry*; Michl, J., Ed.; Kluwer Academic Publ.: Dordrecht, 1997; Vol. 499, pp 287−302.

(2) (a) Rodríguez, M.; Llobet, *A.*; Corbella, M.; Martell, A. E.; Reibenspies, J. *Inorg. Chem.* **1999**, *38*, 2328−2334. (b) Rodríguez, M.; Llobet, A.; Corbella, M. *Polyhedron* **2000**, *19*, 2483.

10.1021/ic025568i CCC: $22.00
Published on Web 10/16/2002

complexes with the Cu_2Cl_2 core, containing also the neutral ligand dialkylpyridine-2,6-dicarboxylate,

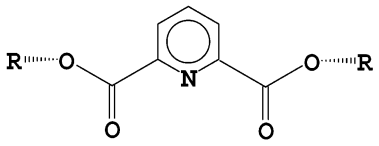

R = Et, depc; R = *i*-Pr, dppc

Depc and dppc are pentadentate ligands that generally act as distorted tridentate meridional ligands through their N atom and through the two carbonyl O atoms from the ester group.[3] These ligands can also be bonded to the metal center by the alkoxy O atoms, although it is a rare coordination mode.[4,5] The two different coordination modes are discussed in the present paper.

Experimental Section

Materials. All reactions were carried out in anhydrous solvents under dry N_2 atmosphere. Solvents were dried using standard techniques (chloroform, dichloromethane, benzene, and toluene over P_2O_5 and THF over sodium pieces and benzophenone). Isopropyl alcohol (Merck) was refluxed over CaO and then distilled and kept over CaH_2. Absolute ethanol (AR quality, Hayman Ltd.) and pyridine-2,6-dicarboxylic acid (Fluka) were used as supplied. Anhydrous $CuCl_2$ was prepared by boiling the hydrated salt under reflux with freshly distilled $SOCl_2$ for about 4 h. The anhydrous $CuCl_2$ was filtered, washed with dry benzene, and dried in vacuo. The diethylpyridine-2,6-dicarboxylate (depc) and diisopropylpyridine-2,6-dicarboxylate (dppc) ligands were prepared according to literature procedures.[6]

[(depc)(Cl)Cu(μ-Cl)$_2$Cu(Cl)(depc)] (1). A solution of anhydrous $CuCl_2$ (1.34 g, 0.01 mols) in THF (25 mL) containing 5 mL of absolute ethanol was added dropwise to a magnetically stirred solution of depc (2.33 g, 0.01 mol) in THF (25 mL). The resulting solution was further stirred for 3 h. On cooling to 0 °C, a yellow brown crystalline solid separated out. It was filtered off, washed with THF (5 mL) and dry petroleum ether (2 × 5 mL), and dried in vacuo. Yield: 2.87 g (80%). Mp: 185−190 °C. Anal. Found: C, 36.68; H, 3.28; N, 3.66; Cl, 19.4. Calcd for $C_{11}H_{13}NO_4Cl_2Cu$: C, 36.92; H, 3.64; N, 3.92; Cl, 19.9. IR (KBr pellet, cm^{-1}): 1750 vs, 1710 vs, 1596 m, 1570 w, 1460 m, 1437 m, 1395 m, 1310 vs, 1255 vs, 1185 s, 1163 m, 1150 w, 1130 s, 1085 m, 1025 m, 1010 m, 855 m, 765 m, 720 m, 690 m, 668 m, 517 w, 430 w. Molar conductance (ohm^{-1} cm^2 mol^{-1}): 34 (MeCN) and 0.4 ($PhNO_2$). The diffuse reflectance spectrum of the powdered sample exhibits two bands at 11.7 kK (855 nm) and 20.8 kK (480 nm).

[(dppc)(Cl)Cu(μ-Cl)$_2$Cu(Cl)(dppc)] (2). This complex was prepared under reaction conditions identical to those of the previous reaction except that isopropyl alcohol was used as the reaction medium instead of ethanol and the dppc ligand was used instead of depc. A light peach colored solid compound was obtained. Yield: 76%. Mp: 210 °C. Anal. Found: C, 40.23; H, 4.26; N, 3.42; Cl, 18.1. Calcd for $C_{13}H_{17}NO_4Cl_2Cu$: C, 40.47; H, 4.41; N, 3.63; Cl, 18.4. IR (KBr pellet, cm^{-1}): 1728 vs, 1590 m, 1545 w, 1460 m, 1358 m, 1305 s, 1270 vs, 1185 m, 1150 m, 1100 s, 1020 m, 955 m, 890 m, 850 m, 830 m, 766 m, 720m, 690 m, 665 m, 430 w. Molar conductance (ohm^{-1} cm^2 mol $^{-1}$): 2.0 (CH_3CN). Its diffuse reflectance spectrum again showed two bands at 11.7 kK and 20.8 kK.

Physical Methods. Elemental analyses (C, H, N) were performed on a Perkin-Elmer model 2400 CHN elemental analyzer. Chlorine was determined by Volhard's method.[7] IR spectra were recorded as KBr pellets on a Perkin-Elmer model 1430 ratio recording spectrometer. The diffuse reflectance spectra of the powdered samples were recorded on a Hitachi 330 UV−vis−NIR spectrophotometer, using $BaSO_4$ as reference. Molar conductances were measured using a Digital conductivity bridge, model CC 601. EPR spectra were monitored with a Bruker ESP 300E. Samples were run at 9.4 GHz (X-band) at 77 K. Variable-temperature magnetic susceptibility measurements in the polycrystalline state were carried out on a Quantum Design MPMS SQUID equipped with a 55 kG magnet in the temperature range 1.8−300 K with an applied magnetic field of 1000 G. Diamagnetic corrections were estimated from Pascal tables (-3.3×10^{-4} for **1** and -3.7×10^{-2} for **2**). Powder X-ray diffraction analysis were carried out in a Siemens D500 automatic diffractometer.

X-ray Crystallography. Crystallization of [(depc)(Cl)Cu^{II}(μ-Cl)$_2$Cu^{II}(Cl)(depc)], **1**, by slow evaporation of its saturated ethanol solution at room temperature yielded good single crystals. Intensity data were collected on a Siemens P4 single-crystal diffractometer equipped with a molybdenum sealed tube (λ = 0.71073 Å) and highly oriented graphite monochromator using crystals of dimensions 0.29 × 0.24 × 0.15 mm mounted in Lindeman glass capillaries. The lattice parameters and standard deviations were obtained by least-squares fit to 40 reflections (9.46° < 2θ < 34.922°). The data were collected by the 2θ−θ scan mode with a variable scan speed ranging from 2.0° to a maximum of 45.0° min^{-1}. Three reflections were used to monitor the stability and orientation of the crystal and were measured after every 97 reflections. Their intensities showed only statistical fluctuations during 18.28 h of X-ray response time. The data were collected for Lorentz and polarization factors, and an empirical absorption correction based on the ψ scan method was applied.

The structure was solved by direct methods using SHELX-97[8] and also refined on F^2 using the same one. All the non-hydrogen atoms were refined anisotropically. The hydrogen atoms were included in the ideal positions with fixed isotropic U values and were riding with their respective non-hydrogen atoms. A weighting scheme of the form $w = 1/[(\sigma^2 F_o^2) + (aP)^2 + bP]$ with $a = 0.0256$ and $b = 0.46$ was used. The refinement converged to a final R value of 0.0249 (wR2 = 0.0654 for 2033 reflections) [$I > 2\sigma(I)$]. The final difference map was featureless. Neutral atom scattering factors and anomalous scattering correction terms were taken from *International Tables for X-Ray Crystallography*.[9]

(3) (a) Schobert, R.; Pfab, H.; Mangold, A.; Hampel, F. *Inorg. Chim. Acta* **1999**, *291*, 91. (b) Davies, J. E.; Mays, M. J.; Raithby, P. R.; Sarveswaran, K.; Shields, G. P. *J. Organomet. Chem.* **1999**, *573*, 180. (c) Wonnemann, J.; Oberhoff, M.; Erker, G.; Frohlich, R.; Bergander K. *Eur. J. Inorg. Chem.* **1999**, *3*, 1111. (d) Wanner, M.; Sixt, T.; Klinkhammer, K.-W.; Kaim, W. *Inorg. Chem.* **1999**, *38*, 2753. (e) Evans, D. A.; Rovis, T.; Kozlowski, M. C.; Tedrow, J. S. *J. Am. Chem. Soc.* **1999**, *121*, 1994.

(4) Birk, R.; Grossmann, U.; Hund, H. U.; Berke, H. *J. Organomet. Chem.* **1988**, *345*, 321−329.

(5) Yoshida, T.; Okano, T.; Otsuka, T.; Miura, I.; Kubota, T.; Kafuku, K.; Nakatsu, K. *Inorg. Chim. Acta* **1985**, *100*, 7−16.

(6) (a) Motekaitis, R. J.; Martell, A. E. *Inorg. Chem.* **1988**, *27*, 2718. (b) Webster, R. D.; Bond, A. M.; Schmidt, T. *J. Chem. Soc., Perkin Trans. 2*, **1995**, 1365.

(7) Volhard, J. *J. Prakt. Chem.* **1874**, *117*, 217.

(8) Sheldrick, G. M. *SHELX-97, Program for the Solution and Refinement of Crystal Structures*; University of Göttingen: Göttingen, Germany, 1997.

Table 1. X-ray Crystallographic Data for Complexes [(depc)(Cl)Cu(μ-Cl)$_2$Cu(Cl)(depc)] (**1**) and [(dppc)(Cl)Cu(μ-Cl)$_2$Cu(Cl)(dppc)] (**2**)

	1	**2**
empirical formula	$C_{11}H_{13}Cl_2CuNO_4$	$C_{13}H_{17}Cl_2CuNO_4$
fw	357.7	385.7
cryst syst	triclinic	monoclinic
space group	$P\bar{1}$	$C2/c$
a, Å	8.3020(10)	11.6360(10)
b, Å	9.2050(10)	25.906(3)
c, Å	10.065(2)	11.7679(10)
α, deg	99.040(10)	90.00
β, deg	100.810(10)	107.900(10)
γ, deg	106.502(10)	90.00
V, Å^3	706.01(18)	3375.4(6)
Z	2	8
T, K	293(2)	293(2)
λ(Mo Kα), Å	0.71073	0.71073
ρ_{calc}, g/cm^3	1.682	1.518
μ, mm^{-1}	1.932	1.623
R	0.025	0.034
R_w[a]	0.065	0.085

[a] $w = 1/[\sigma^2(F_o^2) + (aP)^2 + bP]$ where $P = (\max(F_o^2,0) + 2F_c^2)/3$ with $a = 0.0256$, $b = 0.46$ and $a = 0.0426$, $b = 1.86$ for **1** and **2**, respectively.

The data collection procedure, structure solution, and refinement for **2** were essentially the same as those for **1**. The parameters associated with this structure are as follows: 40 reflections ($10.26° < 2\theta < 30.29°$) for accurate cell parameter determination, $0.27 \times 0.19 \times 0.17$ mm crystal, a total of 44.03 h of X-ray exposure time, $R = 0.0344$ (wR2 = 0.0848 for 2191 reflections) [$I > 2\sigma(I)$] with $a = 0.0426$ and $b = 1.86$ in the weighting scheme. Full details are presented in Table 1.

Calculations. EPR simulations were performed using the WIN-EPR Simfonia program from Bruker. Molecular orbital calculations were carried out using CACAO (Computer Aided Composition of Atomic Orbitals, PC Beta-Version 5.0, 1998),[10a] a program based on the extended Hückel type of analysis using crystallographic coordinates. In the case of the cobalt complex **3**, which contains the same coordination ligands as **1**, the crystallographic coordinates were taken from ref 11 and the hydrogen atom coordinates were calculated using the AMPAC[10b] program.

Results and Discussion

Synthesis and Structure. The dinuclear copper complexes [L(Cl)Cu^{II}(μ-Cl)$_2$Cu^{II}(Cl)L] (L = depc, **1**; L = dppc, **2**) are obtained in good yield by mixing equimolecular amounts of anhydrous $CuCl_2$ and the appropriate ligand in a THF/EtOH solution as shown in the following equation for the depc case:

$$2CuCl_2 + 2depc \xrightarrow{THF/EtOH} \underset{\mathbf{1}}{[(depc)(Cl)Cu^{II}(\mu\text{-}Cl)_2Cu^{II}(Cl)(depc)]} \quad (1)$$

The crystal structures of complexes **1** and **2** have been determined by means of single-crystal X-ray diffraction analysis. Table 1 contains crystallographic data for complexes **1** and **2**, whereas Table 2 contains their selected bond distances and angles. Figure 1 displays the ORTEP diagram obtained for the molecular structure of complexes **1** and **2**, which crystallize in the triclinic $P\bar{1}$ and monoclinic $C2/c$ space groups with two and eight molecules per unit cell, respectively.

Table 2. Selected Bond Lengths (Å) and Bond Angles (deg) for the Complexes [L(Cl)Cu(μ-Cl)$_2$Cu(Cl)L] (L = depc, **1**; L = dppc, **2**)[a]

complex **1**		complex **2**	
Cu1−Cl1	2.3500(8)	Cu1−Cl2	2.3081(9)
Cu1−Cl1#1	2.2737(7)	Cu1−Cl2#2	2.3099(8)
Cu1−Cl2	2.2519(7)	Cu1−Cl1	2.2413(9)
Cu1−N1	2.031(2)	Cu1−N1	2.070(2)
Cu1−O1	2.485(2)	Cu1−O1	2.403(2)
Cu1−O3	2.347(2)	Cu1−O3	2.620(2)
Cu1−Cu1#1	3.3966(7)	Cu1−Cu1#2	3.4050(7)
C6−O2	1.198(3)	C6−O2	1.317(4)
C6−O1	1.325(3)	C6−O1	1.202(4)
C9−O3	1.202(3)	C10−O3	1.194(4)
C9−O4	1.319(3)	C10−O4	1.327(4)
O3Cu1O1	147.37(6)	O3Cu1O1	145.66(7)
N1Cu1Cl1#1	174.47(5)	N1Cu1Cl2#2	169.95(7)
Cl2Cu1Cl1	176.07(3)	Cl1Cu1Cl2	70.37(3)
Cl1#1Cu1Cl1	85.46(3)	Cl2#2Cu1Cl2	4.72(3)
Cl2Cu1Cl1#1	94.84(3)	Cl1Cu1Cl2#2	3.48(3)
N1Cu1Cl2	90.37(6)	N1Cu1Cl1	91.49(7)
N1Cu1Cl1	89.21(6)	N1Cu1Cl2	91.79(7)
N1Cu1O3	76.34(7)	N1Cu1O3	71.01(8)
Cl2Cu1O3	95.57(5)	Cl1Cu1O3	87.78(6)
Cl1#1Cu1O3	104.90(5)	Cl2#2Cu1O3	17.89(5)
O3Cu1Cl1	88.13(6)	O3Cu1Cl2	84.74(6)
Cl2Cu1O1	90.71(5)	Cl1Cu1O1	96.81(6)
N1Cu1O1	71.61(7)	N1Cu1O1	74.85(8)
Cl1#1Cu1O1	106.42(5)	Cl2Cu1O1	92.79(6)
Cl1Cu1O1	85.45(5)	Cl2#2Cu1O1	95.87(5)
Cu1#1Cl1Cu1	94.54(3)	Cu#2Cl2Cu1	95.01(3)

[a] Symmetry transformations used to generate equivalent atoms: #1 ($-x + 1, -y, -z + 1$) and #2 ($-x, y, -z + 1/2$).

Complex **1** possesses an inversion center, and each Cu metal atom has a distorted octahedral coordination. The equatorial plane can be regarded as formed by the two Cl bridging ligands, the terminal Cl ligand, and the N atom from depc. The axial positions, which are significantly bent due to the restrictions imposed by the depc ligand geometry, would then be occupied by the ester oxygen atoms (O3Cu1O1 angle is 147.4°). It is interesting to note the unsymmetric coordination of the depc ligand toward each copper center, using the O3 carbonyl oxygen atom of the ester group in one of the axial positions and the O1 ethoxy oxygen atom in the other. Furthermore as expected, the carbonyl oxygen atoms form slightly stronger bonds with the Cu center than the sp^3 ethoxy oxygens (the Cu−O3 distance is 2.347 Å while the Cu−O1 distance is 2.485 Å).

The dinuclear complex **1** can be globally regarded as two distorted octahedrons sharing the basal edge that contain the bridging chloro ligands (Cl1). The four atoms of the Cu_2Cl_2 core lie in a plane which forms a dihedral angle of 4.2° with the plane formed by the copper center, the terminal chloro ligand, and the N atom from the pyridylic ligand (N1CuCl2) atoms. The Cu_2Cl_2 core has a rhomboidal geometry with two long Cu−Cl distances (Cu1−Cl1 2.350 Å, trans to the terminal Cl2 ligand) and two short Cu−Cl distances (Cu1−Cl1a 2.274 Å, trans to the pyridylic N1 atom). The core bond angles are Cl1Cu1Cl1a 85.5° and CuClCu1a 94.5°. Finally

(9) *International Tables for X-Ray Crystallography*; Wilson, A. J. C., Ed.; Kluwer Academic Publishers: Dordrecht, 1992; Vol. C, pp 500−502, 219−222, and 193−199.
(10) (a) Mealli, C.; Proserpio, D. M.; Ienco, A. *J. Chem. Educ.* **1990**, *67*, 399. (b) AMPAC 6.55 Program, 1997 Semichem, 7204 Mullen, Shawnee, KS 66216.
(11) Singh, G.; Sowerby, D. B. *J. Chem. Soc., Dalton Trans.* **1977**, 490.

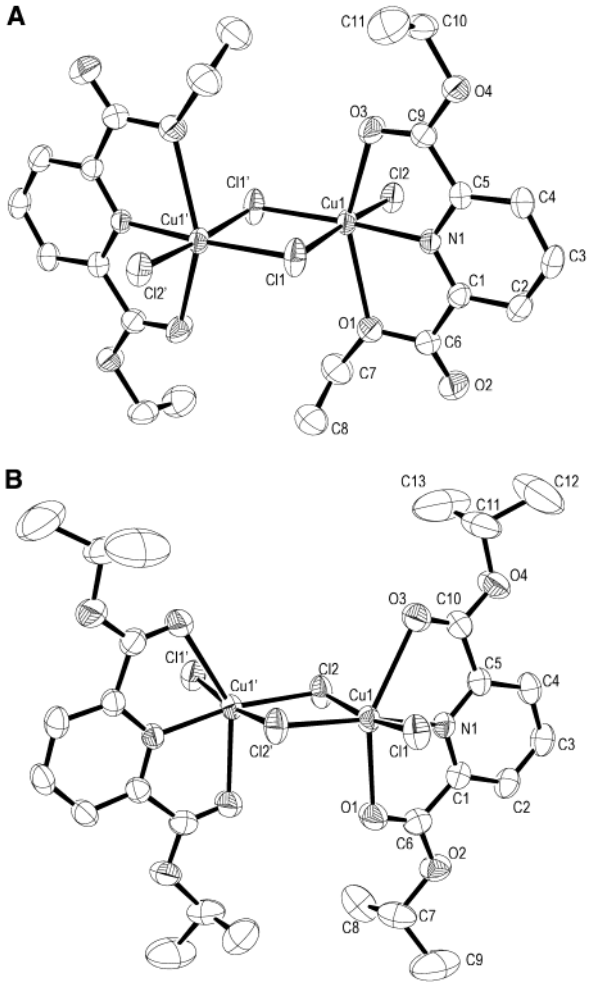

Figure 1. An ORTEP view (ellipsoids at 50% probability) of the molecular structure of (A) [(depc)Cu(μ-Cl)$_2$Cu(depc)] (**1**) and (B) [(dppc)Cu(μ-Cl)$_2$Cu(dppc)] (**2**).

the meridional depc ligands are nearly planar, and they are disposed in a parallel manner with respect to one another (the angle between the pyridyl rings is 0.0°).

The crystal packing of the molecule takes place so that the plane of the core is nearly parallel to the *xz* direction and piles up in a parallel fashion along the *y* axis. The orientation of the cores along the *x* and *z* directions remains unchanged.

The terminal coordination of an ester group to a transition metal center can a priori take place through the carbonyl sp^2 oxygen atom or through the alkoxy sp^3 oxygen atom. In the majority of the cases (see ref 3 for recent examples) the former coordination is obtained since it is favored both from a steric and also from an electronic viewpoint, the carbonyl group having the chance to form significant bonding through its π orbitals.

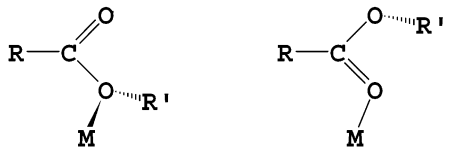

To our knowledge there are only two fully characterized examples in the literature where an ester coordinates through its alkoxy oxygen atom; one of them is an Fe(II)[4] complex whereas the other one is a Rh(I).[5] In both cases, besides the ester group, the ligands contain olefinic groups directly bonded to the metal center. For the Rh(I) complex case, a two-electron-accepting olefinic group is also bonded to the metal and is thought to be responsible for the unusual Rh−O alkoxy coordination.[5]

Complex **1** is the first example described in the literature of a nonorganometallic complex where an ester group coordinates through the sp^3 alkoxy ester oxygen atom. It is also the first example described so far where each arm of the depc ligand coordinates in a different manner, that is, one through the carbonyl oxygen and the other through the sp^3 one.

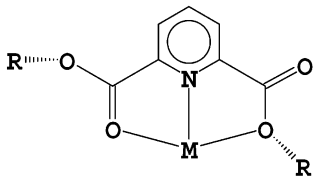

Vibrational spectroscopy is also in agreement with the present structure. In the free ligand, the carbonyl stretching frequency appears at 1730 cm^{-1}, while for **1** it splits in two: one of them shifted to higher energy at 1750 cm^{-1} and the other one shifted to lower energy at 1710 cm^{-1}. This phenomenon can be interpreted as a result of the unsymmetric coordination of the dpec ligand into the copper metal center. The O-sp^3 ester coordination gives rise to a positive shift therefore favoring the Lewis scheme I, whereas the opposite is observed for the carbonyl ester coordination, which favors the Lewis scheme II producing a negative shift.

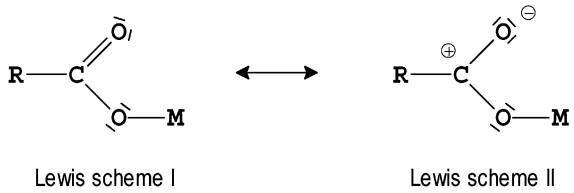

Structurally Related Complexes. Figure 2 and Table 3 present comparative data with structurally related complexes, namely, [(dppc)(Cl)Cu^{II}(μ-Cl)$_2$Cu^{II}(Cl)(dppc)], **2**, and [(depc)(Cl)Co^{II}(μ-Cl)$_2$Co^{II}(Cl)(depc)], **3**. Complex **2** is the analogous Cu complex where the ethyl ester group has been simply substituted by the bulkier isopropyl group in the pyridinedicarboxylate ligand. This produces an enhancement of steric effects that in turn favors the O-sp^2 carbonyl coordination over the O-sp^3 alkoxy. Indeed, in complex **2** only the former type of bonding is observed. The dppc ligand also produces significant structural distortions of the first coordination sphere and particularly of the Cu$_2$Cl$_2$ core as depicted in Figure 2 and quantitatively presented in Table 3. Whereas in complex **1** the Cu$_2$Cl$_2$ core is perfectly planar, in **2** the bridging Cl atoms are moved 0.1 Å above that plane (furthermore the Cu1Cl1Cl1′Cu1′ dihedral angle of 7.6° gives an idea also of the degree of distortion from planarity) thus forming a butterfly-like core. Another significantly different

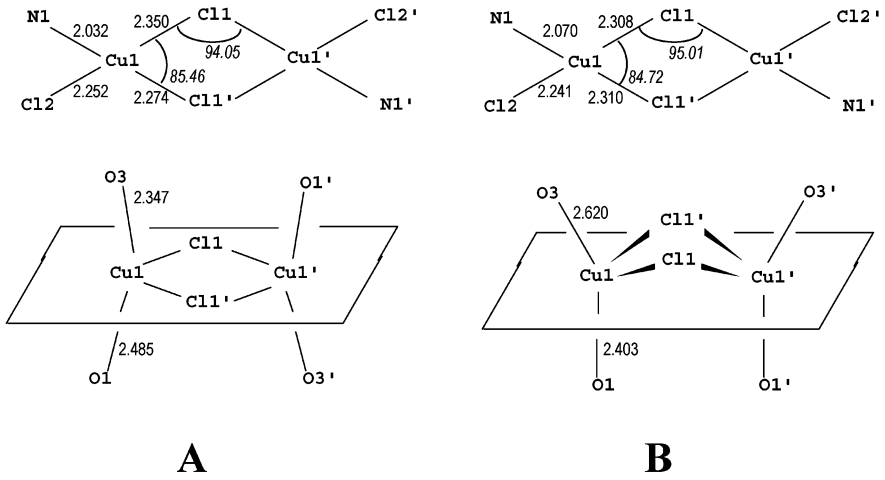

Figure 2. Schematic comparative drawing of molecular structures together with selected structural parameters for **1** (A) and for **2** (B).

Table 3. Comparative Structural Parameters for Complexes **1**−**3**

structural parameters[a]	**1**	**2**	**3**
Cu1−Cl1Cu1′−Cl1′	0	5.2	0
Cu1−Cl1Cl1′−Cu1′	0	7.6	0
N1Cl2−Cu1−Cl1Cl1′	4.2	13.2	3.9
N1−Cl2Cl1−Cl1′	1.7	12.8	3.1
N1Cl2Cu1−Cu′Cl2′N1′	0	27.4	0
N1−Cl2Cl2′−N1′	0	29.6	0
aromatic rings[b]	0	4.9	0
Cl distance from core[c]	0	0.1	0
O1−O3′	4.3	3.6[d]	4.3
O1′−O3	4.3	5.5[e]	4.3
O1Cu1Cu1′	98.6	92.1	98.7
O3Cu1Cu1′	97.6	108.2	96.5

[a] Angles are reported in degrees whereas distances are in angstroms. Torsion angles: between the dashes are indicated the atoms that are shared by both planes. In the case of **3**, it is related to Co. [b] Dihedral angle between the aromatic rings. [c] Shortest distance of the Cl1 atom from the core plane. [d] Equivalent O1−O1′ distance for **2**, see Figure 2. [e] Equivalent O3−O3′ distance for **2**, see Figure 2.

structural feature engendered by the dppc ligand is the N1Cl2−Cu1−Cl1Cl1′ dihedral angle; while this angle is 4.2° for **1**, in **2** it raises up to 13.2°. Those two structural differences have substantial influences into the frontier orbital compositions and energies and thus in turn will generate significant variations in their magnetic behavior (vide infra). Another interesting structural difference for these two complexes is the relative disposition of the pyridinedicarboxylate ligand. In **1**, their aromatic rings are parallel to one another, whereas in **2**, they are tilted by 4.3°. Finally, in complex **1** the depc ligands are situated so that the ethylic repulsions reach a minimum value; thus the difference in their O1Cu1Cu1′ and O3Cu1Cu1′ angles is 0.9°. In sharp contrast, in **2** the equivalent difference is of 16.1°, which can be envisioned as due to a relative rotation of their dppc ligands through a hypothetical axis that would be contained in their respective Cl2Cu and Cl2′Cu′ bonds.

Complex **3** is the homologous complex bearing the same depc ligand but where the Cu metal center has been replaced by cobalt. Now in **3**, all the ester groups coordinate through the O-sp^2 atom in contrast with the heterogeneous type of coordination described above for **1**. Even though the depc ligand in **3** acts in a different manner, the core structural parameters and the cobalt equatorial coordination are remarkably similar to those of **1** (see Table 3). Thus in this case, the O-sp^2 carbonyl coordination is favored over the O-sp^3 because of electronic factors described in the following section.

Theoretical Calculations. We have carried out a theoretical analysis of the complexes **1**−**3** at the extended Hückel (EH) level using the CACAO program,[10a] in order to understand the uncommon coordination behavior of **1** and also to be able to find out the molecular orbitals involved in the superexchange pathway in **1** and **2**. Figure 3 shows frontier orbitals for complexes **1**−**3** obtained at this calculation level.

The EH calculations performed for **1** and **2**, show a near degeneracy for frontier orbitals with an energy gap of only 0.001 eV for compound **1** and 0.041 eV for compound **2**. Those orbitals are well above (2.049 eV for **1** and 1.914 eV for **2**) fully occupied orbitals. The SOMO and SOMO + 1 orbitals for both complexes are depicted in Figure 3A and Figure 3B. As can be observed, the major contributions to the frontier orbitals come from the atoms located in the equatorial plane of the distorted octahedron. This situation is similar to that of the coplanar square-base geometry, previously described in the literature.[2b] The Cu metal centers use $d_{x^2-y^2}$ type orbitals for a σ^* interaction with the p_N and p_{Cl} orbitals of the plane. It is interesting to underline here the significance of the change of symmetry of the "SOMO + 1" and "SOMO" when going from compound **1** to compound **2**. For compound **1**, we are close to the situation where the Cu1−Cl1−Cu1′ angle and the dihedral angle Cu1-(Cl1−Cl1′)Cu1′ are such that the two orbitals are nearly degenerate.[2b,13]

The cobalt complex **3** presents an octahedral environment for each cobalt center relatively similar to **1** (vide supra) except that the Co−O bond distances are significantly much shorter. For complex **3**, a high-spin Co(II) complex, there are three unpaired electrons in each metal site and thus three pairs of SOMOs are expected. This is nicely reflected in the

(12) Kapoor, P.; Pathak, A; Kapoor, R.; Venugopalan, P. *Transition Met. Chem.*, submitted.
(13) (a) Castell, O.; Miralles, J.; Caballol, R. *Chem. Phys.* **1994**, *179*, 377. (b) Khan, O. *Molecular Magnetism*; VCH: New York, 1993; p 162.

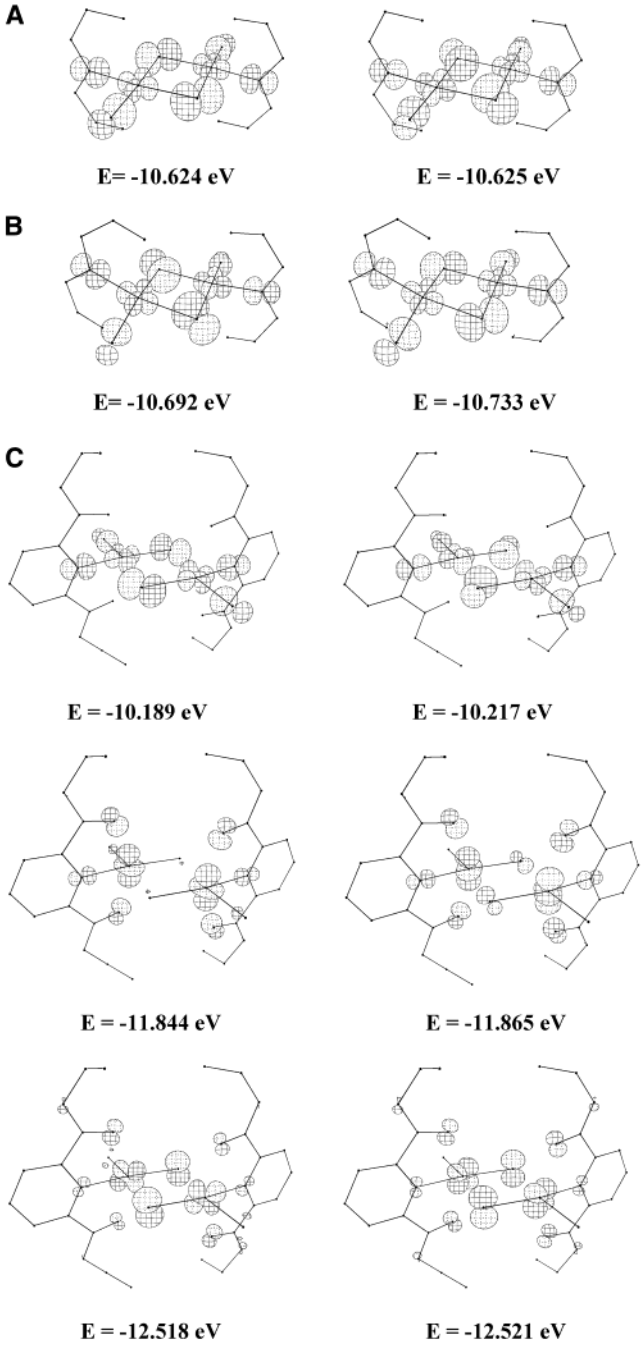

Figure 3. Drawings of SOMOs frontier orbitals (for orbitals contributing more than 1%) obtained for complexes **1** (A), **2** (B), and **3** (C). See text for details.

energies and orbital shapes of the EH calculations depicted in Figure 3C. The highest energy pair of SOMOs are similar to those found for the corresponding Cu complex **1** where the metal complex uses mainly $d_{x^2-y^2}$ type orbitals (see Figure 3C, top). For the lowest energy pair of SOMOs the metal center uses t_{2g} type orbitals (Figure 3C, bottom) whereas for the pair in between it uses d_{z^2} (Figure 3C, middle).

In the series of complexes [(depc)(Cl)M^{II}(μ-Cl)$_2$$M^{II}$(Cl)-(depc)] (M = Mn, Co, Ni, and Cu), the metal center coordinates through the O-sp^2 oxygen atoms except for the Cu complex,[11] where both types of coordination are observed. In order to assess the degree of M−O bonding, the ROP (reduced overlap population[10a]) was calculated for the complexes **1**−**3**, and the values are given in Table 4. From Table 4 it can be inferred that the carboxylate ligand binds more strongly to the Co metal center than to Cu. This is in agreement with the frontier orbital system just described, since t_{2g} type and d_{z^2} type orbitals, which are directly involved in metal center−carboxylate bonding, are singly occupied in the Co complex and fully occupied in the Cu complex. This decreases the antibonding character of the Co−O interaction with respect to the Cu−O bond in complexes **1** and **2**. Table 4 also shows that in the particular case of Cu−depc the O-sp^2 bond is stronger than the O-sp^3.

Table 4. Reduced Overlap Population for M−O Bonds in Complexes **1**−**3**[a]

	M−O═C ROP		M−OR ROP		∑(ROP)[b]
Cu−depc	0.037	(2.347)	0.021	(2.485)	0.116
Cu−dppc	0.030	(2.403)			
	0.009	(2.620)			0.078
Co−depc	0.118	(2.216)			
	0.103	(2.244)			0.442

[a] The corresponding M−O bond distances in angstroms are indicated in parentheses. [b] ∑(ROP) is defined as the summation of all ROP in the complex.

The higher ROP found for Co than Cu is due to both a decrease of the volume of the 3d orbitals, which in turn produces a decrease of the effective orbital overlap with the ligand system, and a progressive increase of electron density in these metal orbitals when going from Mn to Cu. As a result, for the Cu metal complex case the extra stabilization energy gained by the potential ligand π-donor bonding vanishes and therefore both types of oxygen coordination become similarly accessible. The crystal structure of **2**, where the ethyl group has been substituted by the bulkier isopropyl group, elegantly shows how, in this particular case, the increase of steric demands drives the Cu coordination toward the O-carbonyl of the ester group. Furthermore, a decrease of the steric demands (for R = Me) produces the same coordination pattern as for **1**.[12]

This higher bonding strength for the cobalt complex is also reflected in short Co−O bonding distances with regard to the Cu complexes (for **1**, the average Cu−O is 2.415 Å, whereas for **3**, the average Co−O is 2.230 Å).

Magnetic Properties. Figure 4 presents a graph of the molar $\chi_M T$ product vs T for compounds **1** and **2**. At 300 K the values of $\chi_M T$ are ≈0.9 cm^3 K mol^{-1} and increase slowly up to 100 K, at which point the increase proceeds at a much faster pace, reaching a maximum value of 1.100 cm^3 K mol^{-1} at 16.50 K for compound **1** and 1.094 cm^3 K mol^{-1} at 17.50 K for **2**. This behavior is due to a ferromagnetic coupling between the two Cu(II) metal centers. Under ≈17 K, the $\chi_M T$ values decrease, indicating the presence of antiferromagnetic intermolecular interactions, ZFS, or both contributions.

The experimental data were fitted considering the spin Hamiltonian, $H = -JS_1 \cdot S_2$. In order to fit also the decrease of $\chi_M T$ at low temperature, a new J' parameter was introduced, according to the description of intermolecular

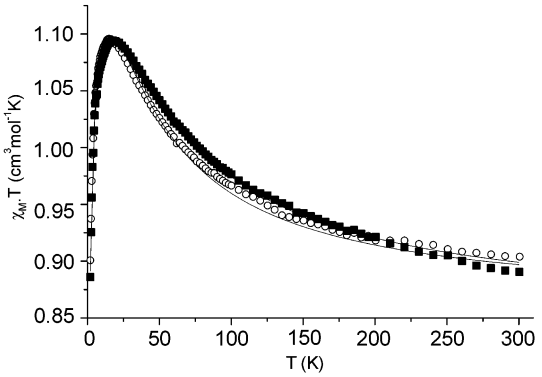

Figure 4. $\chi_M T$ vs T experimental data for **1** (○) and **2** (■) (cm^3 K mol^{-1}). The solid line shows the best fit obtained (see text).

interactions proposed by Kahn.[1c] Thus we used the following Bleaney−Bowers equation for a binuclear compound with a total spin $S = 1$, $\chi_M T = N\beta^2 g^2 T\, F(J,T)/[kT - J'F(J,T)]$, with $F(J,T) = 2(3 + \exp(-J/kT))^{-1}$ where J' includes the dimer−dimer interactions and ZFS. The fit was obtained by minimizing the function $R = \sum(\chi_M T_{calc} - \chi_M T_{obs})^2/\sum\chi_M T_{obs})^2$. The best fit parameters found were, for compound **1**, $J = 39.9(6)$ cm^{-1}, $J' = -0.59$ cm^{-1}, $g = 2.14$, and $R = 2 \times 10^{-5}$ and, for compound **2**, $J = 51.3(5)$ cm^{-1}, $J' = -0.57$ cm^{-1}, $g = 2.13$, and $R = 8.6 \times 10^{-6}$. These values are in agreement with the small SOMO−(SOMO + 1) energy gap calculated by EH and also with the type and degree of structural distortions suffered by complexes **1** and **2**.

The higher J value for **2** is attributed to the nonplanarity of the Cu_2Cl_2 core, in agreement with previous work described in the literature for a family of $Cu_2Cl_6^{2-}$ related anionic complexes.[13a]

Figure 5A and Figure 5B display the powder electron paramagnetic resonance (EPR) spectra for complexes **1** and **2** at 77 K, together with their mathematical simulations. The spectrum of compound **1** shows a narrow band centered at 3100 G, and a large one between 2500 and 3670 G. Another signal can be observed at lower fields (700 G). Using a Gaussian line shape, the simulation parameters obtained for this spectrum at 77 K are as follows: $g_x = 2.11$, $g_y = 2.12$, $g_z = 2.21$, $D = 500$ G (4.67 10^{-2} cm^{-1}), $E = 235$ G (2.19 10^{-2} cm^{-1}) with line widths of 80, 300, and 1100 G in the x, y, and z directions. Applying these parameters to the equations of Wasserman et al.[14] for a triplet ground state, and taking into account that the EPR spectrum for compound **1** was registered at $\nu = 9.4016$ GHz (X-band), this equation yields the following six $\Delta M_s = 1$ transitions: $H_{x1} = 3263$ G, $H_{y1} = 2597$ G, $H_{z1} = 2578$ G, $H_{x2} = 3067$ G, $H_{y2} = 3736$ G, and $H_{z2} = 3486$ G.

For compound **2**, only the central band, around $g = 2$, was observed (no band is observed in the $g = 4$ region). This band shows a slight split at its maximum. Using a Gaussian line shape, the simulation parameters obtained for this spectrum at 77 K are as follows: $g_x = 2.17$, $g_y = 2.16$, $g_z = 2.06$, $D = 195$ G, $E = 0$ G with line widths of 130, 130, and 180 G in the x, y, and z directions. Applying these parameters to the equations of Wasserman et al.[14] for a triplet ground state, and taking into account that the EPR spectrum for compound **2** was registered at $\nu = 9.4024$ GHz (X-band), this equation yields the following six $\Delta M_s = 1$ transitions: $H_{x1} = 3005$ G, $H_{y1} = 3019$G, $H_{z1} = 3072$ G, $H_{x2} = 3185$ G, $H_{y2} = 3200$ G, and $H_{z2} = 3451$ G.

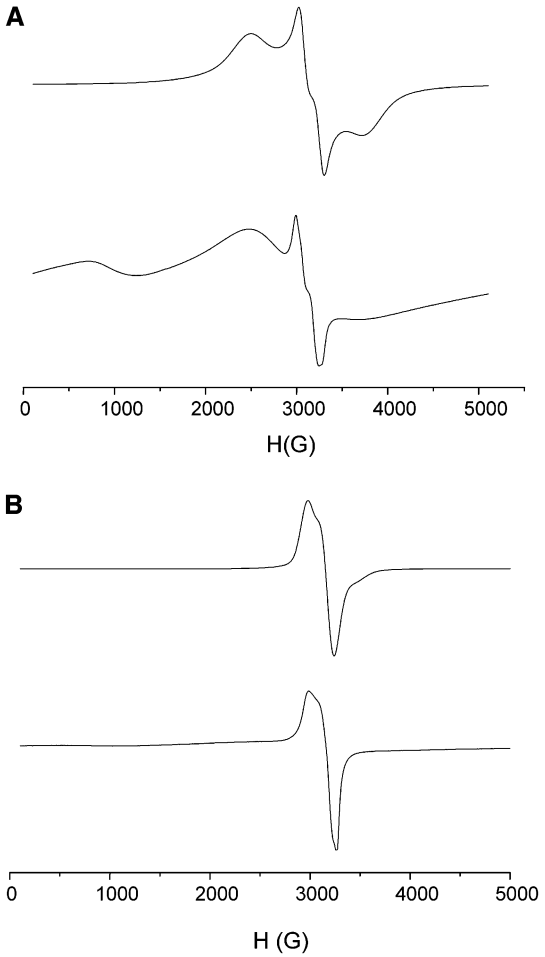

Figure 5. Powder ESR spectra at 77 K (lower graph) together with simulated spectra (upper graph) for complexes **1** (A) and **2** (B).

It is worth mentioning here that the g average obtained from the EPR simulation in the case of complex **2** is identical to the value obtained from χ_M vs T measurements whereas in the case of complex **1** it is very close (2.14 from magnetic measurements vs 2.15 from EPR spectrum). These values manifest the consistency of the overall magnetic data treatment presented here related to complexes **1** and **2**.

Conclusions

Complex [(depc)(Cl)$Cu^{II}(\mu\text{-}Cl)_2Cu^{II}$(Cl)(depc)], **1**, presents a situation similar to that of the coplanar square-base geometry, from both structural and magnetic points of view. Thus it has a planar Cu_2Cl_2 core, and its magnetic properties can be structurally correlated with previous examples described in the literature. Furthermore, this complex is of interest because it is the first example where the ester group is bonded to the metal center through both O-alkoxy and O-carbonyl ester atoms in an alternate manner. The presence of the *i*-Pr group in [(dppc)(Cl)$Cu^{II}(\mu\text{-}Cl)_2Cu^{II}$(Cl)(dppc)],

(14) Wasserman, E.; Snyder, L. C.; Yager, W. A. *J. Chem. Phys.* **1964**, *41*, 1763.

2, produces significant structural and electronic distortions. Now **2** has a butterfly-like Cu_2Cl_2 core which changes magnetic properties with regard to the coplanar type of complexes mentioned above. In addition, the bulkier *i*-Pr groups also produce a change in the coordination modes of the ester group giving rise to only carbonyl O-sp^2 type coordination, due to steric effects. It is interesting to note that the related Co(II) complex with the depc ligand, [(depc)-(Cl)Co^{II}(μ-Cl)$_2$Co^{II}(Cl)(depc)], **3**, also coordinates only through the carbonyl O-sp^2 atoms. Theoretical analysis together with structural data clearly show that in the present case a much stronger M−O carbonyl bond is formed than in the related Cu(II) cases, thus avoiding an alkoxy O-sp^3 type of coordination with its potentially unfavorable steric effects.[15]

(15) A CIF containing all crystallographic information for complexes **1** (CCDC #179225) and **2** (CCDC #179226) is available.

Acknowledgment. P.K. and P.V. thank Panjab University, Chandigarh, for financial support through the UGC unassigned grant (minor research project). This research has also been financed by MCYT of Spain through Projects BQU2000-0458 and BQU2000-0791. A.L. is grateful to CIRIT Generalitat de Catalunya (Spain) for the Distinction award and the aid SGR2001-UG-291. J.R. acknowledges partial support from CONACYT (Mexico) and the Visiting Professors Grant (Comissionat per a Universitats i Recerca del Departament de la Presidència de la Generalitat de Catalunya) and is grateful for useful discussions with Miquel Sola and for hospitality during a sabbatical visit at the Institut de Química Computacional and the Department of Chemistry of the University of Girona, Spain.

IC025568I